6. R. M. Goody, *Atmospheric Radiation*, vol. 1, *Theoretical Basis* (Clarendon, Oxford, 1964).
7. N. S. Alvi, C. E. Backus, G. W. Masden, in *Proceedings of 12th Photovoltaic Specialists Conference* (IEEE, New York, 1976), p. 948; J. J. Loferski, in *ibid.*, p. 957.
8. G. W. Masden and C. E. Backus, in *Proceedings of 13th Photovoltaic Specialists Conference* (IEEE, New York, 1978), p. 853; R. L. Moon, L. W. James, H. A. Vanderplas, Y. G. Chai, G. A. Antypas, in *ibid.*, p. 859; A. Bennett and L. C. Olsen, in *ibid.*, p. 868; M. F. Lamorte and D. Abbott, in *ibid.*, p. 874; J. A. Cape, J. S. Harris, R. Sahai, in *ibid.*, p. 881; L. M. Fraas and R. C. Knechtli, in *ibid.*, p. 886; A. G. Milnes, in *ibid.*, p. 892; M. Arienzo and J. J. Loferski, in *ibid.*, p. 898.
9. J. J. Loferski, *J. Appl. Phys.* **27**, 777 (1956).

4 December 1978; revised 1 March 1979

Galápagos Hydrothermal Mounds: Stratigraphy and Chemistry Revealed by Deep-Sea Drilling

Abstract. *The Galápagos mounds sea-floor hydrothermal system is at least 300,000 years old and once produced manganese-poor sediments, which nearly blanketed the area of the present mounds field. Present-day mound deposits are limited manganese-rich exposures, suggesting that the system has changed from rock- to water-dominated and has diminished in intensity with time.*

In May 1977 the drilling ship *Glomar Challenger*, during Deep Sea Drilling Project (DSDP) leg 54, found and cored small mounds of sea-floor hydrothermally produced sediments in an area of high heat flow 22 km south of the Galápagos Rift (*1*, *2*). A deep tow survey had shown the mounds to be arrayed in rows, strips, and ridges above small, near-vertical basement faults, and to be up to 10 m high and 25 m in diameter (*3*). They also have high water temperatures; have surfaces consisting of dark Fe-Mn oxides, brown to yellow iron oxyhydroxides, and clay minerals; and support thriving communities of macrobenthos (*4*).

The drilling provided the first complete sediment sections through any sea-floor hydrothermal deposits and reached basaltic basement in four places, penetrating as much as 45 m below the sediments in one hole. We have already presented data (*5*) on the composition of the sediments and basalts cored in the four holes at DSDP site 424, showing the sediments to be similar to reported hydrothermal deposits from the Mid-Atlantic Ridge (*6*) and the Gulf of Aden (*7*). Here, we explore the consequences of the stratigraphy and transition metal chemistry of the deposits.

The four holes were drilled along a north-south line and spaced about 300 m apart (Fig. 1). Holes 424 and 424A were directly on mounds, and hole 424B was in a flat area between them. Hole 424C was not completely cored beacuse of time constraints, but provided an undisturbed "mud-line" core (the top 10 cm are oxidized surface sediments), allowing us to reconstruct the sediment profile (Fig. 1) from the deep tow survey (*3*) by using water depths determined by drill-string length (rather than acoustically). This confirmed that we had cored two elevated mound structures in holes 424 and 424A.

Three types of sediments were recovered: (i) dark gray, semilithified, soft but brittle Fe-Mn oxides and clays; (ii) a distinct green mud, consisting almost entirely of Fe-rich, Mn-poor smectites (*5*); and (iii) foraminifer-nannofossil ooze with a moderate siliceous component (Fig. 1). This represents the stratigraphic sequence in the two holes on mounds. The process of drilling severely mixed the dark gray and green sediments at the top of the two holes, but individual chips of the dark gray material consist of two mineralogic end-members, Fe-Mn oxides (mainly todorokite with some birnessite) and Fe-rich, Mn-poor clay minerals identical to the more uniform green muds deeper in the holes. Green muds form discrete thin beds in holes 424 and 424A and a bed several meters thick in hole 424B, sandwiched between two layers of foraminifer-nannofossil ooze (Fig. 1); these contain no manganese oxides. About 12 to 15 m of foraminifer-nannofossil ooze occurs at the base of holes 424, 424A, and 424B.

Hole 424B is important because it represents the regional sediment blanket, which is uniformly about 25 to 30 m thick in the area. Two reflectors in this sediment blanket, thought to be ash layers, were found by the deep tow survey (*3*). However, hole 424B has no ash layers. Instead, the top and bottom of the green mud layer in that hole provide sufficient acoustic impedance contrasts (the muds are about 30 percent denser than the calcareous oozes) to explain the reflectors. Consequently, we believe that the green muds at hole 424B represent a nearly continuous layer between older and younger calcareous oozes throughout the area of the mounds field [about 350 km^2 (*1*, *3*)]. The age of basement at site 424 estimated from sea-floor magnetics (*1*) and shipboard biostratigraphy is about 600,000 years. Assuming a uniform carbonate sedimentation rate (*8*) and an effectively "instantaneous" rate for the nearly carbonate-free green muds, the deepest green muds in hole 424B (15 m above basement) were first deposited about 300,000 years ago. The basal reflector pinches out about 12 km from the Galápagos Rift on crust about 300,000 years old [assuming uniform sea-

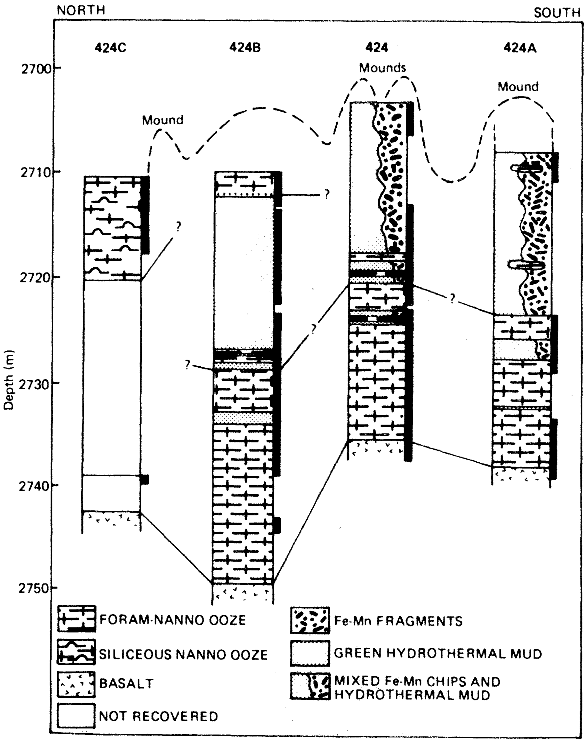

Fig. 1. Lithologic columns for holes 424, 424A, and 424C (sediments and top of basement only). Columns to the right of each lithologic column show recovery for each core, with the recovered interval beginning at the top of each core (DSDP convention). Lithologic boundaries have been placed by assuming that the core recovery is representative of the entire 9.5-m interval of each core.

floor spreading (*1*, *3*)], the same age as the base of the green muds predicted by stratigraphic means (*9*). If the cause of the reflector that far north is the same layer of green mud, then the hydrothermal field was once much larger than the present area of the mounds.

The arrangement of the mounds in chains and ridges above basement faults originally suggested that the faults served as pathways for source hydrothermal solutions leaking from the crust (*3*). Basaltic basement directly beneath two mounds, however, is fresh. Only traces of clay mineral alteration occur in the basalts. Combined water (H_2O^+) in 29 basalt samples measured on board *Glomar Challenger* ranged from 0.3 to 1 percent. The Fe_2O_3/FeO ratio is also low, averaging 0.43 ± 0.008 (*5*). Either basement vents beneath the mounds are very narrow ($\lesssim$ 5 m) and we missed them, or there is no direct vertical connection between the mounds and actual active hydrothermal vents. The basement relief may simply provide zones of weakness in the sediment blanket, localizing the exit of dispersed hydrothermal fluxes. The mounds may in part be piercement structures, with the green mud layer arched upward over basement faults by more recent hydrothermal activity (including flow of hot water and addition of new material). Deep tow profiles show that, indeed, the two reflectors in the sediments arch upward toward the centers of mounds (*3*).

High concentrations of Mn (10 to 30 percent) compared with other trace metals [Ni, Co, Cu, and Zn, which are present at only tens to a few hundred parts per million (ppm)] distinguish these and other sea-floor hydrothermal deposits from typical manganese nodules or basalt encrustations (*5*, *10*). The green muds are virtually free of $CaCO_3$ and have high iron (24 to 31 percent calculated at Fe_2O_3) but low Al_2O_3 (1 to 2 percent), manganese (0.1 to 0.3 percent calculated as Mn_3O_4), and transition trace metals (Ni, Co, Cu, and Zn levels of 10 to 100 ppm); this distinguishes them from pelagic clays (*10*), which are largely derived from windblown dust and volcanic material, both high in Al. Element ratios such as Mn/Al and (Ni + Co + Cu)/Mn can thus be used to monitor the input of hydrothermally derived manganese relative to both "pelagic clay-manganese nodule" and terrigenous inputs to the sediment column, and they eliminate the dilution effect of biogenic carbonate and silica (Fig. 2).

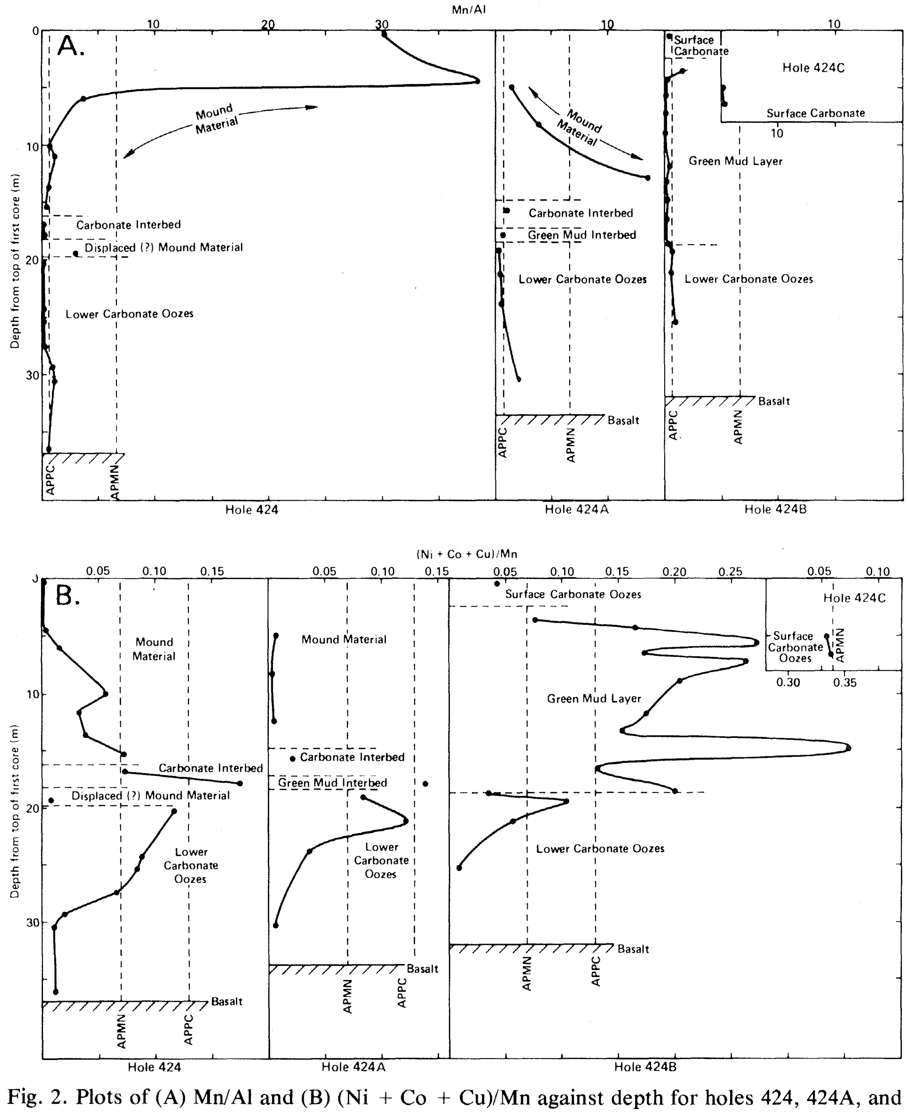

Fig. 2. Plots of (A) Mn/Al and (B) (Ni + Co + Cu)/Mn against depth for holes 424, 424A, and 424C. Data are from Hoffert *et al.* (*20*). Depth intervals were assigned by assuming that core recovery is representative of the entire 9.5-m interval of each core. Abbreviations: *APPC*, average Pacific pelagic clay (*10*) and *APMN*, average Pacific manganese nodule (*21*).

Hole 424 has the least disturbed sequence of mound materials. The drop of Mn/Al with depth (Fig. 2A) to levels similar to those in the green mud layer of hole 424B shows how surficial the Mn-rich deposits are. The shallowest green muds in hole 424 are at the level of the upper carbonate ooze in hole 424B; the mounds are thus cored with green mud, derived from the more widespread green mud layer.

In all three holes, Mn/Al increases in the lowest 10 m of carbonate and (Ni + Co + Cu)/Mn drops (Fig. 2B). There is thus no preferential enrichment of hydrothermal Mn at the bases of the two mound holes that have drastically higher surficial Mn/Al. This is stronger evidence than basalt freshness that hydrothermal flux is not along basement faults immediately beneath mounds; it must be elsewhere. Instead, we believe that the modest Mn enrichment in the basal carbonate reflects ridge-crest hydrothermal activity. Hydrocasts and near-bottom sampling at the Galápagos Rift 22 km north of site 424 show a steady increase in dissolved and particulate Mn downward in the water column, culminating in distinct plumes of hot water emanating from fissures at the axis of spreading (*11*). The residence time of this Mn in the Panama Basin is about 50 years and its mean dispersal distance is 1000 km (*12*). Thin deposits of reddish brown or orange presumed ferromanganese oxides have been photographed (*13*) near where the hot-water plumes were sampled. Because of the low velocities of bottom currents throughout the Panama Basin (*14*), the amount of Mn deposited at one place in the sediments should diminish as the site moves away from the rift by sea-floor spreading. This is what we believe happened at site 424.

About 300,000 years ago, however, the site was far enough away from the Galápagos Rift, and its underlying igneous rocks were cool and thick enough to allow seawater fairly deep access in the crust. A major hydrothermal system developed which may have deposited green muds over a much wider area than the present mounds field, but at least nearly blanketed the entire area of the mounds field. Because the green muds are so free of Mn oxides and form discrete beds a few centimeters to several meters thick, the mounds stratigraphy implies that the surficial mounds Mn oxides were deposited later. We do not think that the Mn oxides were "fractionated" from the green muds during an interval of simultaneous deposition. Nor do we believe that the present high surface abundance of Mn oxides results from their having been leached or remobilized from buried green muds. Instead, we propose that the mounds stratigraphy and the probably widespread green mud layer imply an evolution of the Galápagos mounds sea-floor hydrothermal system. Early in its history, voluminous Mn-poor sediments were deposited as flat-lying beds. Today, Mn-rich materials are being deposited in a smaller area of restricted outcroppings, the mounds.

Experiments tracing the alteration of basalts in varying proportions of seawater show that in rock-dominated systems (high rock/water ratios), metals initially dissolved from the rock are soon reprecipitated as alteration minerals in the rocks. This occurs as Mg, the most important element extracted from seawater to form secondary minerals, becomes depleted in circulating hydrothermal fluids (*15*). In this model, the amount of metal in solution is buffered. The *p*H is low (and metals stay in solution) during Mg extraction. The *p*H increases when Mg is depleted in the fluids and hydrolysis of silicates become pronounced. In water-dominated systems, Mg is never completely extracted from the circulating fluids; the *p*H remains low and metals stay in solution. In these systems, the rocks become almost completely altered, and Mg extraction is limited by the volume of rock interacting with hydrothermal fluids.

We propose that the Galápagos hydrothermal system was initially rock-dominated because deep crustal rocks were fresh and hydrothermal circulation had just begun to reach them. As the system became established and rocks more altered, it became water-dominated and more and more soluble metals reached the sea floor. In its rock-dominated phase, Mg-Fe silicates were deposited over exhalative vents. In its most recent water-dominated phase, Fe-Mn oxides have become more abundant.

Alternatively or simultaneously, a decrease in volume of hydrothermal solutions reaching the sea floor may have affected the composition of the hydrothermal deposits. For particular experimental hydrothermal solutions, mixture with seawater will cause precipitation of (i) amorphous silica, (ii) Mg layer-lattice silicates, or (iii) pure ferric oxyhydroxides as seawater dilution increases from 1:1 to 1:39 (*15*). The green muds and Fe-Mn deposits of the mounds may be analogs of (ii) and (iii), respectively. The greater abundance of Fe-Mn oxides in the most recent deposits could then reflect a lower flow rate of hydrothermal solutions reaching the sea floor. The difficulty with this hypothesis is that huge volumes of hydrothermal solutions would have been needed to reduce bottom waters sufficiently to delay precipitation of Mn as the widespread green muds were deposited. Unless such solutions could have been ponded as brines, this is unlikely. The green mud layer, traced with seismic reflectors, is too uniform in thickness and too widespread (*3*) and basement relief is too low and lineated (*1*) for ponding to have occurred.

Finally, the change from deposition of Fe-rich, bedded green muds 300,000 years ago to Mn oxides in the present mounds may partly reflect a recent increase in the oxygen level of Panama Basin bottom waters. Efficient segregation of Mn from Fe can occur in solutions moving through a relatively reducing milieu (*16*); Fe-Mn oxides precipitate when oxygen availability is higher. The green color of the clays apparently reflected the presence of Fe^{2+} in the solutions from which they precipitated (*17*) on the sea floor. The precise chemical conditions are difficult to estimate because the *p*H and the activities of certain anions (such as bicarbonate) may affect Fe and Mn solubilities (*18*). We note that the Panama Basin is virtually enclosed (*19*) and suggest than an increase in bottom-water residence time or even temporary density stratification may have occurred if colder, denser, and more voluminous bottom waters entered the Panama Basin via the Peru-Chile trench (*12*) at times in the Pleistocene. Oxygen depletion would have occurred rapidly in response to equatorial high productivity, allowing Mn to stay in solution in bottom waters while Fe-rich green muds precipitated. Although this is highly speculative, we regard sea-floor hydrothermal materials as the products of complex interactions among igneous rocks, sediments, hydrothermal fluids, and seawater. These subtle interactions could easily be influenced by oceanographic conditions, and this hypothesis better explains the purity of the green muds (Mn-oxide and carbonate-free), their stratification, and their possible lateral extent than other hypotheses so far advanced. In effect, we suggest that a type of basinal, rather than local, ponding may explain these aspects of the deposits.

JAMES H. NATLAND
Scripps Institution of Oceanography,
La Jolla, California 92093
BRUCE ROSENDAHL
Duke University,
Durham, North Carolina 27708
ROGER HEKINIAN
Centre Océanologique de Bretagne,
Brest, France
YURI DMITRIEV
U.S.S.R. Academy of Sciences,
Moscow, Soviet Union
RONALD V. FODOR
North Carolina State University,
Raleigh 27607
ROBERT M. GOLL
Duke University,
Beaufort, North Carolina 28516
MICHEL HOFFERT
Université Louis Pasteur,
Strasbourg, France
SUSAN E. HUMPHRIS
Lamont-Doherty Geological
Observatory,
Palisades, New York 10964
DAVID P. MATTEY
University of Birmingham,
Birmingham, United Kingdom
NIKOLAI PETERSEN
Ludwig-Maximilians-Universität,
Munich, Federal Republic of Germany
WILLIAM ROGGENTHEN
South Dakota School of Mines and
Technology, Rapid City 57701
EDWARD L. SCHRADER
University of Alabama,
Tuscaloosa 35486
RAMESH K. SRIVASTAVA
Rajasthan University, Udaipur, India
NICK WARREN
University of California,
Los Angeles 90024

References and Notes

1. K. D. Klitgord and J. D. Mudie, *Geophys. J. R. Astron. Soc.* **38**, 563 (1974).
2. J. G. Sclater and K. D. Klitgord, *J. Geophys. Res.* **78**, 6951 (1973); D. L. Williams, R. P. Von Herzen, J. G. Sclater, R. N. Anderson, *Geophys. J. R. Astron. Soc.* **38**, 587 (1974); J. G. Sclater, R. P. Von Herzen, D. L. Williams, R. N. Anderson, K. D. Klitgord, *ibid.*, p. 609.
3. P. Lonsdale, *Earth Planet. Sci. Lett.* **36**, 92 (1977).
4. J. B. Corliss, M. Lyle, J. Dymond, K. Crane *ibid.* **40**, 12 (1978).
5. R. Hekinian *et al.*, *Oceanologia Acta* **1**, 473 (1978).
6. M. Hoffert, A. Perseil, R. Hekinian, P. Choukroune, H. D. Needham, J. Francheteau, X. LePichon. *ibid.*, p. 73; R. B. Scott, P. A. Rona, L. W. Butler, A. J. Nalwalk, M. R. Scott, *Nature (London) Phys. Sci.* **239**, 77 (1972); M. R. Scott, R. B. Scott, P. A. Rona, L. W. Butler, A. J. Nalwalk, *Geophys. Res. Lett.* **1**, 355 (1974).
7. J. R. Cann, C. K. Winter, R. G. Pritchard, *Mineral. Mag.* **41**, 193 (1977).
8. N. G. Pisias, *Geol. Soc. Am. Mem. 145* (1976), p. 375.

9. W. D. Bukry, *Init. Rep. Deep Sea Drilling Project*, in press.
10. D. S. Cronan, *Geochim. Cosmochim. Acta* **33**, 1562 (1969).
11. G. Klinkhammer, M. Bender, R. F. Weiss, *Nature (London)* **269**, 319 (1977).
12. P. Lonsdale, *Deep-Sea Res.* **24**, 1065 (1977).
13. R. F. Weiss, *Earth Planet. Sci. Lett.* **37**, 257 (1977).
14. P. Lonsdale, *Geology* **5**, 147 (1977).
15. W. Seyfreid and J. Bischoff, *Earth Planet. Sci. Lett.* **37**, 71 (1977).
16. K. B. Krauskopf, *Geochim. Cosmochim. Acta* **12**, 61 (1957).
17. H. Harder, *Chem. Geol.* **18**, 169 (1976).
18. J. M. Hein, *Geol. Soc. Am. Bull.* **83**, 443 (1972).
19. P. Lonsdale and K. D. Klitgord, *ibid.* **89**, 981 (1978).
20. M. Hoffert, A. Courtois, A. M. Karpoff, D. Trauth, unpublished data from leg 54.
21. D. S. Cronan, in *Ferromanganese Deposits on the Ocean Floor*, D. R. Horn, Ed. (Lamont-Doherty Geological Observatory, Palisades, N.Y., 1972), p. 19.
22. Reviews by and/or discussions with Jerris Gieskes, James Bischoff, Michael Arthur, and Peter Lonsdale are gratefully acknowledged. This is contribution M-636 of the Scientific Department of Centre Océanologique de Bretagne.

5 October 1978; revised 23 February 1979

Chemical Warfare Agents: Verification of Compounds Containing the Phosphorus-Methyl Linkage in Waste Water

Abstract. *The chemical analysis of the waste water from plants that manufacture chemicals is a nonintrusive method for confirming a suspected violation of the prohibition against the production of chemical warfare agents. The chemical structure of most nerve gases is related to that of methylphosphonic acid, whereas most organophosphorus pesticides have the phosphoric acid structure. On the basis of this characteristic difference, a procedure has been developed in which the presence of a nerve gas, its decomposition products, or its starting materials in waste water (Rhine River and Meuse River water) is reflected by the appearance of methylphosphonic acid as a breakdown product after hydrolysis. This acid is concentrated and converted into a volatile compound by methylation. After cleanup, the ester may be separated from related compounds by gas chromatography and is detected by means of a specific detector for phosphorus. The detection limit of nerve gases by this procedure is approximately 1 nanomole per liter of water. The scope and limitations of the method are discussed.*

Since chemical warfare was initiated with the use of chlorine gas in World War I, a large number of candidate chemical agents has become available. Their characteristics vary considerably, and among them one finds irritants, vesicants, suffocating agents, paralyzants, psychochemicals, defoliants, and extremely toxic nerve gases. Recently a review on proven or alleged instances of the use of chemical warfare agents has been published (*1*).

As a result of the massive use of some of these agents during World War I, the Geneva Protocol of 1925 was established, prohibiting the (first) "use in war of asphyxiating, poisonous or other gases" (*2*, p. 69). Because of ambiguities in the text of the Protocol, the Secretary-General of the United Nations called upon all countries to reach agreement to halt the development, production, and stockpiling of all chemical (and biological) agents for purposes of war (*2*). Discussions on such a treaty started in the Conference of the Committee on Disarmament in Geneva in 1969.

Many countries consider an adequate verification of such a production ban a prerequisite for the treaty. The main function of an effective verification system is to deter the production of chemical warfare agents, in particular the most dangerous. To achieve adequate deterrence, procedures are necessary to ensure that there is a reasonable probability that clandestine production will be detected. Clearly, the least intrusive verification methods are preferred.

A variety of methods has been proposed to confirm a suspected violation of the prohibition (*3*), including economic monitoring, satellite observation, and analysis of atmospheric, liquid, and solid waste samples. Among these, in addition to direct liquid waste analysis, the nearsite inspection of river water downstream of chemical production plants showed particularly interesting possibilities.

In 1977 the Dutch delegation to the Conference of the Committee on Disarmament presented a working paper (*4*) on the verification of the presence of nerve gases, their decomposition products, or their starting materials in river water as a model for waste water. Because of their extreme toxicity, the nerve gases constitute the most serious threat among chemical warfare agents. Apart from very small quantities used in medicine these compounds do not seem to have any legitimate use. The nerve gases (**I**) are organophosphorus compounds and are structurally related to pesticides (**II**). Both types of compounds may be prepared in similar production plants. However, there is an important structural difference between these compounds. Most of the nerve gases are related to methylphosphonic acid (**III**), whereas most of the commercially available organophosphorus pesticides have phosphoric acid (**IV**) as their basic structure. A few experimental pesticides (*5*-*7*) are based on structure **III**.

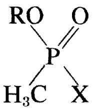

I

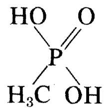

III

Examples of structure **I** include VX, in which R = C_2H_5 and X = $SCH_2CH_2N(i\text{-}C_3H_7)_2$, and Sarin, in which R = $i\text{-}C_3H_7$ and X = F.

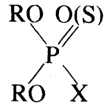

II

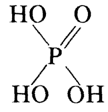

IV

An example of structure **II** is parathion, in which R = C_2H_5, X = $OC_6H_4NO_2$-*p*, and P=O(S) becomes P=S.

The Japanese delegation to the Conference of the Committee on Disarmament has drawn attention (*8*) to the fact that the phosphorus-carbon bond is not cleaved under mild decomposing conditions. Moreover, Milly (*9*, p. 172) stated that, no matter what type of treatment is used on the discharge, it will be most unlikely that all characteristic components will be destroyed. Compounds containing phosphorus-methyl linkages, for example, will almost certainly persist and be identifiable for long periods after discharge. Gas chromatography in combination with specific phosphorus detection was proposed by the Japanese delegation as a suitable method for detecting organophosphorus compounds at very low concentrations.

The evaluation of a verification procedure, based on the above-mentioned considerations, is presented here. A more detailed description of the procedure is given in (*10*). Samples from the Rhine and Meuse rivers, both considered to be heavily polluted, were used as models for substantially diluted waste water downstream of chemical production plants. The compound VX was used as a representative of the nerve gases.

The first step in the verification procedure consists of the hydrolysis of the water sample. After a complete hydrolysis, most phosphorus-containing nerve gases will be converted to methylphosphonic acid, whereas organophosphorus pesticides will hydrolyze to phosphoric acid. In order to establish optimum conditions, we collected hydrolysis data for